

Article

On Some Origins of Tautomeric Preferences in Neutral Creatinine in Vacuo: Search for Analogies and Differences in Cyclic Azoles and Azines

Ewa Daniela Raczyńska

Department of Chemistry, Warsaw University of Life Sciences (SGGW), ul. Nowoursynowska 159c, 02-776 Warszawa, Poland; ewa_raczynska@sggw.edu.pl; Tel.: +48-22-59-37623

Abstract: In order to look for the origins of tautomeric preferences in neutral creatinine in vacuo, we examined prototropic conversions for model azoles, namely mono-hydroxy and mono-amino imidazoles, and also for their selected 1-methyl derivatives. All possible isomeric forms of creatinine and model compounds, resulting from intramolecular proton transfer (prototropy), conformational isomerism about –OH, and configurational isomerism about =NH, were studied in the gas phase (model of non-polar environment) by means of quantum-chemical methods. Because the bond-length alternation is a consequence of the resonance phenomenon, it was measured for all DFT-optimized structures by means of the harmonic oscillator model of electron delocalization (HOMED) index. Important HOMED analogies were discussed for investigated azoles and compared with those for previously studied cyclic azines, including pyrimidine nucleic acid bases. The internal effects were taken into account, and the stabilities of the investigated tautomers-rotamers were analyzed. Significant conclusions on the favored factors that can dictate the tautomeric preferences in creatinine were derived.

Keywords: isomeric transformations in cyclic hetero compounds; change of electron delocalization; HOMED analogies; relative isomer-stability differences; origins of isomeric preferences; DFT search



Citation: Raczyńska, E.D. On Some Origins of Tautomeric Preferences in Neutral Creatinine in Vacuo: Search for Analogies and Differences in Cyclic Azoles and Azines. *Symmetry* **2024**, *16*, 98. <https://doi.org/10.3390/sym16010098>

Academic Editor: Takashiro Akitsu

Received: 22 December 2023

Revised: 9 January 2024

Accepted: 9 January 2024

Published: 12 January 2024



Copyright: © 2024 by the author. Licensee MDPI, Basel, Switzerland. This article is an open access article distributed under the terms and conditions of the Creative Commons Attribution (CC BY) license (<https://creativecommons.org/licenses/by/4.0/>).

1. Introduction

Numerous biomolecules containing heteroatoms (such as N and/or O), and also π - and n-electrons exhibit a particular case of constitutional isomerism of functional groups called prototropic tautomerism [1–4]. Creatinine (**Crea**: $C_4H_7N_3O$, preferred IUPAC name: 2-amino-1-methyl-5H-imidazol-4-one) is one of them. Possessing a heterocyclic structure, in which the acylguanidine part is included in the five-membered ring, **Crea** belongs to the family of glycoyamidines [5,6]. This lactam compound is spontaneously formed in vertebrates from the acyclic nitrogenous organic acid creatine ($C_4H_9N_3O_2$, IUPAC name: 2-[carbamimidoyl(methyl)amino]acetic acid, also called as methylguanidoacetic acid) (Figure 1) [7–10]. The two biomolecules, acyclic creatine and its cyclic anhydride creatinine, possess different isomeric forms, such as prototropic tautomers, and also conformational and configurational isomers [5,11–14]. They play a principal role in the metabolism of proteins [7,9,15]. As the end product of this process, **Crea** is always present in the urine and blood of healthy human organisms in almost constant concentrations that mainly depend on their body weight [9]. Its abnormal level indicates various disease states of muscles and/or kidneys. For detection of renal dysfunction, determination of **Crea**-concentration in urine seems to be a more valuable analysis than that of urea [16].

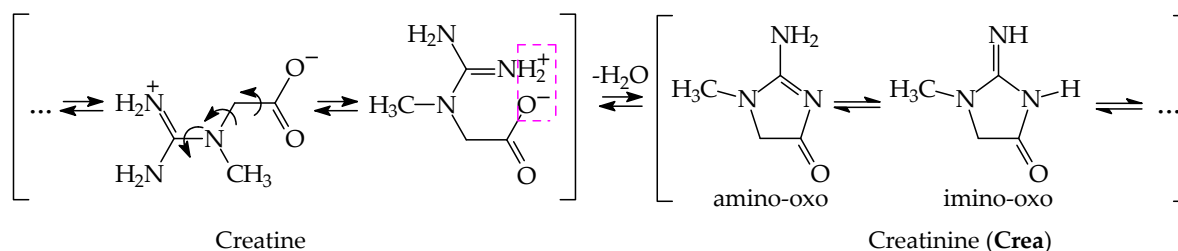


Figure 1. Scheme of reversible transformation between acyclic creatine and cyclic creatinine. Arrows for creatine correspond to isomeric transformations (rotations about single bonds), and arrows for creatinine refer to prototropic conversions (intramolecular proton-transfers).

Already in the 19th century, the significance of creatine and creatinine in the human life has been well recognized [7,17]. This encouraged many chemists and biochemists to undertake various experimental and theoretical studies on their structure and physico-chemical, chemical, and biochemical properties (see for example refs [5–9,11,18–28]). The two derivatives continue attracting the particular attention of researchers even in the 21st century (see for example articles on structural studies [12–14,29–32]). An interesting article was published in 2021 by Léon et al. [14], who discussed spectroscopic and computational results for the favored tautomeric forms of creatinine in the solid state, polar solvents, and gas phase.

Two important tautomers (showed in Figure 1) were detected for **Crea**. The amino-oxo-form is present in the solid state [14,18,26,27,31] as well as in the polar solvents [13,14,22,27–29,32]. The imino-oxo isomer is favored in the gas phase [13,14,22,27,32]. Note that the two tautomers of neutral **Crea** exceptionally possess a C-sp³ atom in the five-membered ring. This means that delocalization of π - and n-electrons in the cycle is incomplete, and the two isomers do not display an aromatic character. In the case of heterocompounds with the six-membered cycle, such as mono-hydroxy and mono-amino pyridines and pyrimidines, as well as di-substituted pyrimidine nucleic acid bases, tautomers containing the C-sp³ atom in the ring can only be classified to the family of rare, and even exceptionally rare forms, similarly as those for phenol and aniline [33]. For neutral cyclic azine-derivatives, these tautomers have never been experimentally identified. They could be studied only theoretically using quantum-chemical methods. Tautomeric mixtures of pyrimidine nucleic acid bases and their model azines consist mainly of tautomers possessing tautomeric protons at heteroatoms. For example, isocytosine (**iC**) contains the –NH₂/=NH group at 2-position and the –OH/=O group at 4-position in the ring; similarly with **Crea**, however, these groups in **iC** are linked to carbons of the six-membered pyrimidine ring, whereas in **Crea** they are attached to carbons of the five-membered imidazole ring. Moreover, the N1-sp³ atom in **Crea** cannot participate in tautomeric conversions and cannot change into N-sp². It contains the Me group that eliminates prototropy. In **iC**, the N1-sp² atom can attach the labile proton and can change its character from =N– (base) to –NH– (acid). These structural differences involve dramatic changes in tautomeric preferences. In the gas phase, **iC** prefers the aromatic amino-hydroxy tautomer [34,35], whereas **Crea** favors the non-aromatic imino-oxo form [13,14,22,28,32].

Looking for the reasons of particular stability of **Crea**-tautomers containing the C-sp³ atom in the five-membered ring, we examined in vacuo, first, the complete tautomeric mixtures for hydroxy- and amino-substituted azoles (**2AIm**, **4AIM**, **2A1MIm**, **2OIm**, **4OIm**, and **4O1MIm**, Figure 2), and next, the complete tautomeric mixture for creatinine (Figure 1). In the literature, one can find some partial results for isolated tautomeric azoles [2,3,36–39], but no general conclusions can be derived. For our examination, we used the same quantum-chemical methods as applied previously for pyrimidine nucleic acid bases and their model aromatic azines [33]. We estimated the stabilities of all possible isomers on the basis of their relative thermochemical parameters. We also measured the power of resonance in individual isomers by means of the geometry-based descriptor, harmonic oscillator model of electron delocalization (HOMED) index [40]. The use of the

same methods for geometry optimization and quantitative analysis of the structural and energetic parameters for individual **Crea**-isomers as well as for their model azoles gives us the possibility to find some reasons for particular stability of **Crea**-tautomers containing the endo-C-sp³ atom. It also makes it possible to compare the computational results for creatinine and the model azoles with those for the previously studied pyrimidine nucleic acid bases and model azines. The comparison of geometric and energetic parameters shows interesting similarities and differences for tautomeric heterocycles possessing the five- and six-membered rings.

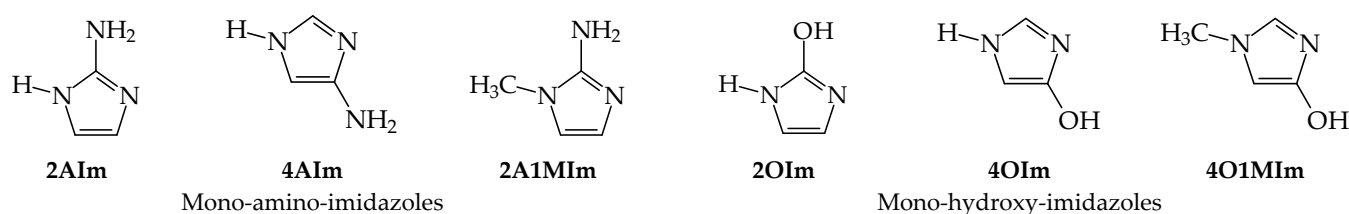


Figure 2. Mono-substituted azoles selected in this work as models for creatinine.

2. Methodology

It should be mentioned here that chemists have frequently considered experimental techniques as exceptionally important methods in investigation of structural phenomena for organic compounds of biological activity. However, for the majority of isomeric systems, only the major and some minor isomers can be detected by means of spectroscopic methods (UV, IR, Raman, MW, MS, NMR, etc.), particularly in the gas phase or solution [1–4,14,33,36]. Most of the minor isomers cannot be distinguished from the background, and rare isomers are usually undetectable. Additionally, isomeric transformations are very fast and reversible processes, and single isomers can be difficult to isolate experimentally. Isomeric equilibria are also very sensitive to their environment, e.g., the presence of other molecule(s), ion(s), and radical(s), as well as changes in phase, solvent, pH, and even the method of vaporization. Fortunately, the complete isomeric mixtures containing major, minor, rare, and exceptionally rare forms can be investigated theoretically by means of quantum-chemical methods.

2.1. Computational Details

Among various theoretical methods employed in acid-base chemistry, particularly for investigation of proton transfer equilibria, we chose the density functional theory (DFT) method [41] with the three-parameter hybrid exchange functional of Becke [42] and the correlation functional of Lee, Yang, and Parr (B3LYP) [43], and larger basis sets with the diffuse and polarization functions [44] as previously described for tautomeric nucleic acid bases and their model compounds [33,45]. The DFT(B3LYP)/6-311+G(d,p) level of theory has been considered as sufficient to describe quantitatively proton-transfer reactions [46,47]. It is also appropriate for analyzes of structural and energetic parameters for other tautomeric compounds containing heteroatoms [45,48].

All possible prototropic tautomers were taken into account in quantum-chemical calculations for **Crea** and model azoles **2AIm**, **4AIM**, **2A1MIm**, **2OIm**, **4OIm**, and **4O1MIm**. Additionally, two zwitterionic forms were considered, one for **4O1MIm** and the other one for **Crea**. The structures of all possible isomers considered here for investigated compounds are shown in Figures S1–S5 (Supplementary Materials). Their geometries were fully optimized at their ground states without symmetry constraints using the DFT(B3LYP)/6-311+G(d,p) level of theory. Only two hydroxy isomers, one of **2OIM** and the other one of **4OIm**, are not found. Structures of all the other isomers of **Crea** and model azoles are stable at the DFT level.

For selected major and minor isomers of **4OIm**, we also applied the Gaussian (G) theories {G2 and G2(MP2)} [49,50], which take considerably more computational time than the DFT methods, but they reproduce sound experimental results. They are recommended

for calculations of energetic parameters of the proton-transfer reactions [51]. The G_n methods were already used for tautomeric organic compounds containing amino and/or hydroxy groups linked to C atoms of the six-membered ring, e.g., mono-hydroxy azines [52] and isocytosine [35]. In most of cases, the DFT and G_n methods led to analogous relative Gibbs energies and isomeric preferences. Some discrepancies occurred for hydroxy- and oxo-tautomers of azines for which the relative Gibbs energies are close to zero [33,52]. Employing the G-theories to **4OIm**, we were able to verify the application of the selected level of theory for tautomeric prediction. For all quantum-chemical calculations, the Gaussian 03 series of programs [53] were applied.

2.2. Structural Descriptor of Electron Delocalization

The geometry-based HOMED index, recently extended to acyclic and cyclic hetero-compounds, properly measure any type of electron delocalization, σ - π hyperconjugation, n - π and π - π conjugation, aromaticity, as well as their various mixtures [40]. Its procedure is analogous to that of the original harmonic oscillator model of aromaticity (HOMA) index [54,55]. The HOMED index for investigated derivatives can be estimated using the same Equation (1) as that proposed earlier for the HOMA index [56] reformulated for homo- and heteroaromatics:

$$\text{HOMED} = 1 - \{\alpha(\text{CC})\Sigma[R_o(\text{CC}) - R_i(\text{CC})]^2 + \alpha(\text{CN})\Sigma[R_o(\text{CN}) - R_i(\text{CN})]^2 + \alpha(\text{CO})\Sigma[R_o(\text{CO}) - R_i(\text{CO})]^2\} / n \quad (1)$$

In this equation, $\alpha(\text{CC})$, $\alpha(\text{CN})$ and $\alpha(\text{CO})$ are the normalization constants, $R_o(\text{CC})$, $R_o(\text{CN})$ and $R_o(\text{CO})$ are the optimum bond lengths for the reference molecules, $R_i(\text{CC})$, $R_i(\text{CN})$ and $R_i(\text{CO})$ are the calculated bond lengths in the studied structures, and n is the number of bonds taken into account in the HOMED estimation. Only the values of the α and R_o parameters are different in the HOMED [40] and HOMA procedure reformulated in 1993 [56]. Parameterization of the HOMED index is based on that of the original HOMA index proposed in 1972 for aromatic hydrocarbons [54] and in 1974 for aromatic heterocycles [55]. For more details on the HOMED parameterization and differences between the HOMED and reformulated HOMA indices, see in the refs [40].

The values of $R_o(\text{CC})$, $R_o(\text{CN})$, and $R_o(\text{CO})$ applied for the optimum CC, CN, and CO bond lengths in the reference molecules (benzene, 1,3,5-triazine, and protonated carbonic acid, respectively) and the values of the corresponding normalization $\alpha(\text{CC})$, $\alpha(\text{CN})$ and $\alpha(\text{CO})$ constants for the odd and even number of bonds considered in the HOMED procedure are summarized in Table 1. All of them were estimated by employing the same level of theory (DFT(B3LYP/6-311+G(d,p)) [40] as that used for the isomers of the investigated model azoles and creatinine. The use of the same quantum-chemical method for determination of the HOMED parameters and for analyzes of electron delocalization in the conjugated tautomeric systems minimize computational errors to the minimum.

Table 1. HOMED parameters employed in this work (taken from Ref. [40]).

Bond	Reference Molecule	R_o (Å)	α_5	α_7	α_6
CC	C ₆ H ₆	1.3943	78.34	80.90	88.09
CN	C ₃ N ₃ H ₃	1.3342	81.98	84.52	91.60
CO	C(OH) ₃ ⁺	1.2811	67.84	69.74	75.00

For all stable isomers of creatinine and for all stable isomers of model azines, the DFT-calculated bond lengths in the optimized structures have been used for quantitative description of electron delocalization measured by the HOMED index. This descriptor was calculated for the five-membered ring (five bonds, $n = 5$), as well as for the entire conjugated molecule-fragment containing the exo-heterogroups (six bonds in **2AIM**, **4AIM**, **2A1MIm**, **2OIm**, **4OIm**, and **4O1MIm**, $n = 6$; and seven bonds in **Crea**, $n = 7$). We used the following abbreviations in this work for the estimated geometry-based index: HOMED5, HOMED6, and HOMED7, respectively. Note that the CH₃ group linked to the endo-N1

atom in **2A1MIm**, **4O1MIm**, and **Crea** does not participate in prototropy. Being a non-conjugated group with tautomeric sites, the H₃C–C bond was not taken into account in the HOMED estimations. However, the lone-pair of n-electrons on N1 can be conjugated with other labile electrons. Hence, the C2N1 and C5N1 bonds were considered in the HOMED5 estimations together with other bonds of the five-membered ring, C2N3, C4N3, C4C5. For the HOMED6 and HOMED7 estimations, the exo-bonds (CN and/or CO) were additionally included. The HOMED values estimated for all isomers possessing the stable DFT-structures are included in Figures S1–S5 (Supplementary Materials).

2.3. Thermochemical Quantities

Thermochemical quantities can be employed for quantitative description of isomeric equilibria, and also for estimation of isomeric mixture compositions. They have been estimated for all isomers after their geometry optimization. For each stable structure, vibrational frequencies and thermochemical quantities such as the electronic energy (E), zero-point energy (ZPE), enthalpy (H , Equation (2)), entropy (S), and Gibbs energy (G , Equation (3) for $T = 298.15$ K) were calculated using the same level of theory (DFT(B3LYP/6-311+G(d,p)) as that applied for the geometry optimization. All positive frequencies found for stable isomers prove that their optimized structures are true minima.

$$H = (E + \text{ZPE}) + pV \quad (2)$$

$$G = H - TS \quad (3)$$

The relative thermochemical quantities (ΔE , ΔH , $T\Delta S$, and ΔG) and equilibrium constants (K , Equation (4)) have been also estimated. The ΔG values include changes in E , ZPE, and thermal corrections to the energy and entropy (vibrational, rotational, and translational contributions). The calculated ΔE , ΔH , $T\Delta S$, and ΔG , and K values quantitatively describe all considered intramolecular transformation: prototropy, conformational and configurational isomerism [1,2,33,36]. Constitutions of the investigated isomeric mixtures have been found on the basis of the estimated K s. Using their values, the mole fractions (x_i , Equation (5), where n is the number of considered isomers) have been determined for all stable isomers (major, minor, rare, and even, exceptionally rare forms) considered in the isomeric mixtures. The estimated values of ΔE , ΔH , $T\Delta S$, ΔG , K , and x_i for all stable isomers are compared with the HOMED indices in Tables S1–S3 (Supplementary Materials).

$$K = \exp(-\Delta G/RT) \quad (4)$$

$$x_i = K_i / (\sum_1^n K_i) \quad (5)$$

3. Results and Discussion

3.1. Possible Tautomers-Rotamers for Model Azoles and Creatinine

For mono-substituted imidazoles containing one exo-NH₂ or OH group in the aromatic forms (**2AIm**, **4AIm**, **2OIm**, and **4OIm** given in Figure 2), two tautomeric protons, one attached to the exo-heteroatom and the other one to the endo-N atom, can move between six conjugated tautomeric sites (N1, C2, N3, C4, C5, and X6). According to the IUPAC prototropy definition [57], 1,3-, 1,5- and/or 1,7-proton shifts are always accompanied by delocalization of π -electrons. Consequently, eight tautomers are possible for each derivative. Their structures are shown in Figure 3. To distinguish the eight tautomers of **2AIm**, **4AIm**, **2OIm**, and **4OIm**, we use the following abbreviations here: **16**, **26**, **36**, **46**, **56**, **13**, **15**, and **34**. They refer to the numbers of two heavy atoms possessing the tautomeric protons. For example, tautomer **16** contains the labile protons at the endo-N1 and exo-X6 atoms. Note that for **2AIm** and **2OIm**, three pairs of tautomers **16** and **36**, **46** and **56**, and also **15** and **34** have identical constitutions. Thus, the number of tautomers, considered in the DFT calculations, is reduced to five. In the case of **4AIm** and **4OIm**, all eight tau-

tomers possess different constitutions, and all of them have been taken into account in the DFT calculations.

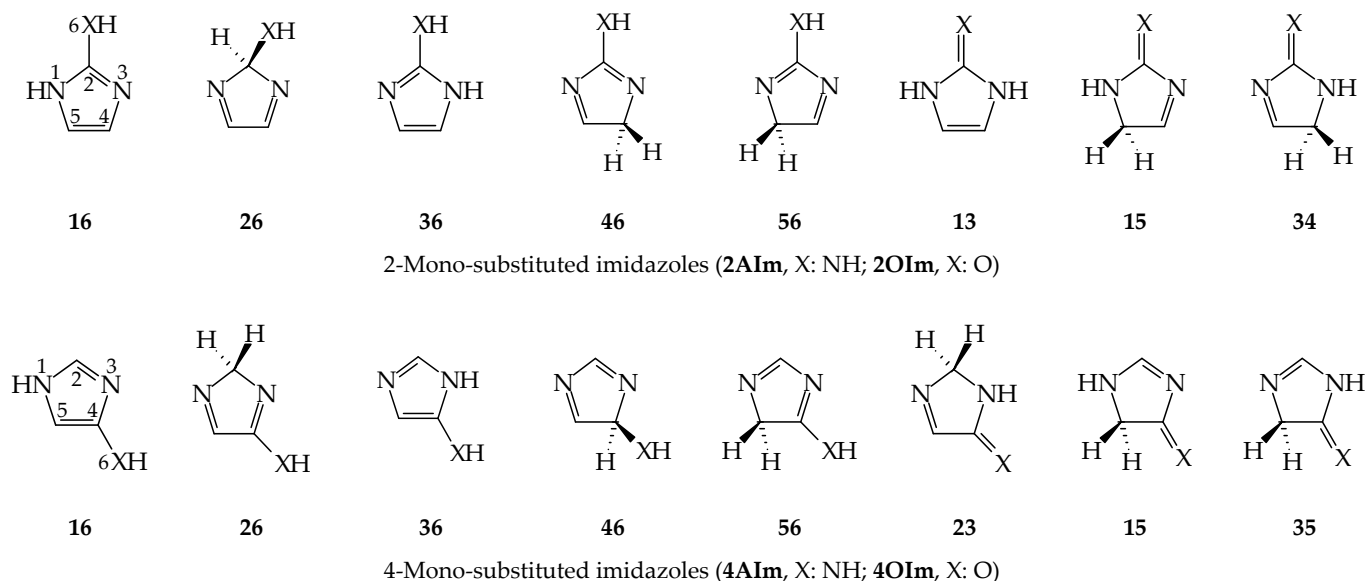


Figure 3. Structures of all possible prototropic tautomers for mono-substituted imidazoles.

The 1-methyl derivatives **2A1MIm** and **4O1MIm** contain only one tautomeric proton linked to the exo-heteroatom in the aromatic forms (Figure 2). It can move between three and two conjugated sites, respectively. The presence of Me at the endo-N1 atom reduces prototropic equilibria in the imidazole ring. Some of those that are possible for mono-substituted imidazoles (Figure 3) are impossible for 1-methyl derivatives (Figure 4). Consequently, the tautomeric mixture of **2A1MIm** consists of three tautomers (6, 3, and 5), while only two tautomers (6 and 5) are possible for **4O1MIm**. All of them possess different constitutions.

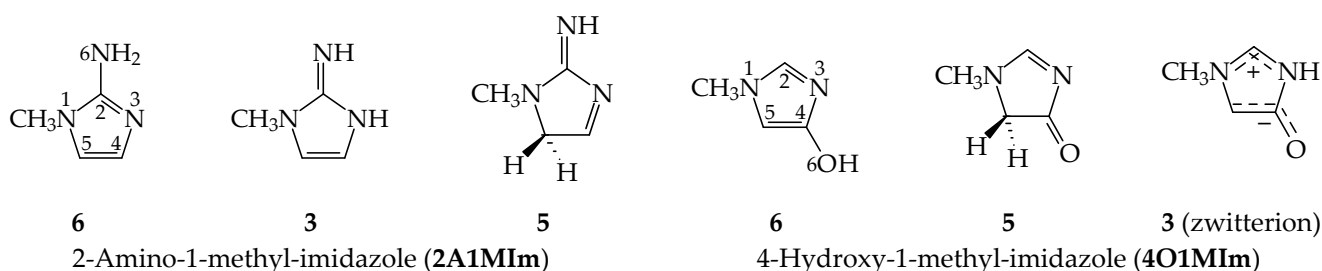


Figure 4. Isomers considered in this work for mono-substituted 1-methyl-imidazoles.

For **2A1MIm** and **4O1MIm**, the tautomer abbreviation correspond to the number of heavy atom possessing the labile proton. The zwitterionic form **3** (possible for **4O1MIm**) with separation of the positive and negative charge, like in amino acids, also has a different constitution. It can be formed from **6** or **5** during intramolecular proton transfer from the exo-O6H or endo-C5H group to the endo-N3 atom. According to the IUPAC prototropy definition [57], the zwitterionic form **3** cannot be considered as a prototropic tautomer, because the acid (O6H and C5H) and base (N3) sites, participating in this internal neutralization reaction, are not conjugated.

Since conformational isomerism about $-O6H$ can additionally takes place in the hydroxy tautomers, two extreme rotational isomers (**a** and **b**) can be considered for **16**, **26**, **36**, **46**, and **56** in the isomeric mixtures of **2OIm** and **4OIm**, and also for **6** in the isomeric mixture of **4O1MIm**. For the imino forms, configurational isomerism about $=N6H$ can

also lead to two extreme geometric isomers (**a** and **b**). They are possible for **13**, **15**, and **34** in the **2AIm** mixture, for **23**, **15**, and **35** in the **4AIm** mixture, and also for **3** and **5** in the **2A1MIm** mixture. In consequence, the following numbers of tautomers-rotamers have been considered in the DFT calculations for the model azoles: six for **2AIm**, eleven for **4AIm**, eight for **2OIm**, thirteen for **4OIm**, five for **2A1MIm**, and three for **4O1MIm** (see structures in Figures S1–S4, Supplementary Materials).

We found that only two tautomers-rotamers of mono-hydroxy-imidazoles (**2OIm-16a/36b** and **4OIm-36a**) do not possess stable structures. The repulsion between the endo $>N1H$ or $>N3H$ and exo $-O6H$ groups possible in **2OIm-16a/36b** and **4OIm-36a** is so high that $-O6H$ rotates about $C-O$ during the geometry optimization to the other, more stable conformer (**2OIm-16b/36a** and **4OIm-36b**, respectively). Structures of all other tautomers-rotamers of the model azoles are stable at the DFT level. In the literature, isomers containing the $C-sp^3$ atom in the five-membered ring have been frequently neglected for azoles. To our knowledge, there are only a few documents discussing their stability for unsubstituted imidazole and for some its derivatives (see refs [3,36,45,48,58–60]).

Creatinine (**Crea**) can be considered as derivative of 1-methyl-imidazole containing two tautomeric exo-groups, NH_2 and OH at the 2- and 4-position (see amino-hydroxy form **67** in Figure 5). It possesses two tautomeric protons, but only four conjugated tautomeric sites ($N3$, $C5$, $N6$, and $O7$). Thus, according to the IUPAC prototropy definition [57], the two labile protons of the exo-groups can move to the conjugated tautomeric sites at the 3- and 5-positions together with migration of π -electrons, and we can additionally write four prototropic tautomers (one amino-oxo **56**, two imino-hydroxy **37** and **57**, and one imino-oxo form **35**) that result from the biomolecule internal property, keto-enol, amine-imine (amidine), enamine-imine, and amide-iminol transformations. Intramolecular proton transfer (acid-base reaction) in **Crea** can also form the zwitterionic form (**36**). For abbreviations of creatinine tautomers, we used the numbers of atoms to which the tautomeric protons are linked, like for model azoles. Additionally, the $=N6H$ and $-O7H$ groups can take two extreme configurations (**a** and **b**) and two extreme conformations (**a** and **b**), respectively. Consequently, two isomers (**a** and **b**) are possible for tautomers **67** and **35**, whereas four isomers (**aa**, **ab**, **ba**, and **bb**) can be considered for **37** and **57**. Hence, thirteen tautomers-rotamers and one zwitterionic form **36** (see structures in Figure S5, Supplementary Materials) were taken into account in our DFT calculations.

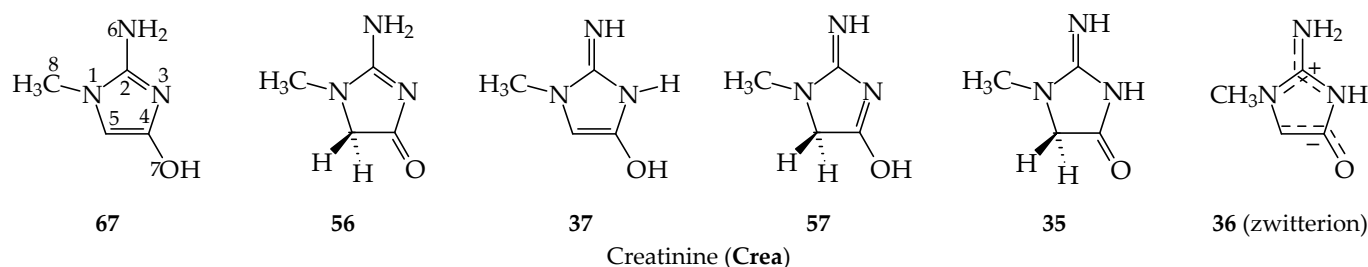


Figure 5. Prototropic tautomers and zwitterionic form possible for creatinine.

In the literature, mainly the amino-oxo and imino-oxo tautomers have been considered in theoretical and experimental investigations [11,21,22,27–32]. Recently, Valadbeigi and coworkers [13], employing quantum-chemical methods, investigated nine isomers of creatinine, including some amino-hydroxy and imino-hydroxy tautomers-rotamers, and even the zwitterionic form. However, no complete information can be derived from their investigation on the stability order of all thirteen possible **Crea**-isomers. It is true that Léon et al. [14] analyzed all tautomers-rotamers for creatinine, but finally they neglected all hydroxy isomers in spectral studies and considered only the amino-oxo (**56**) and imino-oxo isomers (**35a** and **35b**). Note that the zwitterionic form (**36**) has not been considered in aqueous solution [14].

3.2. Variations of Structural-Descriptor HOMED for Isomers of Investigated Derivatives

The first perusal of the HOMED indices calculated at the DFT level for all stable isomers of **2AIm**, **4AIm**, **2OIm**, **4OIm**, **2A1MIm**, and **4O1MIm** (Figures S1–S4 in Supplementary Materials) shows that the HOMED values are between 0.8 and 1.0 for aromatic forms containing the amino or hydroxy group (**2AIm-16/36**, **4AIM-16**, **4AIM-36**, **2OIm-16b/36a**, **4OIm-16a**, **4OIm-16b**, **4OIm-36b**, **2A1MIm-6**, **4O1MIm-6a**, and **4O1MIm-6b**). Generally, HOMEDs for the aromatic forms are higher for the 4- compared to the 2-substituted derivatives. Additionally, HOMED5s describing electron delocalization in the five-membered ring are higher than HOMED6s referring to the entire delocalized system. The imidazole ring contains six labile electrons (four π -electrons and two n-electrons) and it is aromatic, like in other azoles [40], whereas the entire delocalized system consisting of the imidazole ring and the exo N6H₂ or O6H group possesses eight labile electrons, i.e., extra two n-electrons of N6 or O6. This cross n- π and π - π conjugation of the eight labile electrons in the entire conjugated system leads to weaker electron delocalization compared to the conjugation of the six labile electrons in the aromatic ring.

For the imino and oxo tautomers-rotamers without C-sp³ in the ring (**2AIm-13**, **2OIM-13**, **2A1MIm-3a**, and **2A1MIm-3b**), HOMEDs are also slightly higher for the five-membered ring than for the entire conjugated part. Generally, they are close to 0.7. Analogous HOMEDs (close to 0.7) are found for the zwitterionic form **4O1MIm-3**. However, in this case, the value for HOMED5 is slightly lower than that for HOMED6 (without N1–Me bond), suggesting that the separation of the delocalized positive and negative charges in the zwitterion system containing the exo-heterogroups increases the alternation of bond lengths in comparison to that in the five-membered ring. All the imino, oxo, and zwitterionic forms (without endo-C-sp³) can be considered as moderately delocalized isomers in comparison to the aromatic ones. As could be expected, the other isomers (possessing endo-C-sp³) completely lose an aromatic character of the ring. Owing to the cross σ - π hyperconjugation with n- π and π - π conjugations, all of them have weakly delocalized structures. Their HOMED5 and HOMED6 values are not higher than 0.4.

Analogous variations of the HOMED indices (HOMED6 and HOMED7) have been observed previously for tautomeric mono-amino and mono-hydroxy pyrimidines (azines) containing the six-membered ring with N included at the 1- and/or 3-positions [33]. However, the HOMED values are slightly higher than those for azoles. They are close to unity for the aromatic forms (>0.9), for which the six-membered ring contains six labile π -electrons. Usually, aromatic derivatives with only π -electrons are better delocalized than those possessing a mixture of n- and π -electrons in the ring, like aromatic azoles [40]. For the imino and oxo forms of azines without C-sp³ in the ring, the HOMED values are between 0.7 and 0.8, and for those containing the endo-C-sp³ atom are lower than 0.5. Slightly higher HOMEDs for isomers of azines are a consequence of higher numbers of π -electrons and lower numbers of n-electrons in the conjugated parts than in the case of investigated isomers of azoles. This tendency is in accord with the general rules of resonance that are well recognized in organic chemistry. The resonance structures with a separation of positive and negative charge are less important in the resonance hybrid of n- π and π - π conjugated parts than those without separation of charge in only π - π conjugated systems. More important resonance structures in the resonance hybrid involve stronger electron delocalization in the conjugated system.

However, independently on the type and power of conjugation, the HOMED variations for isomers of 2-amino imidazoles are parallel to those for the corresponding isomers of 2-hydroxy derivatives. In the other words, analogous intramolecular proton transfers (1,3-, 1,5-, or 1,7-proton shifts) involve analogous electron delocalization in **2AIm** and **2OIm**. The same is true for **4AIm** and **4OIm**. Changes of the HOMED5 and HOMED6 values are symmetric (see Figures S6 and S7, Supplementary Materials). Thus, general linear relationships (Figure 6) exist between HOMED5s, and separately, between HOMED6s estimated for all stable isomers of mono-amino (**AIm**) and mono-hydroxy imidazoles (**OIm**).

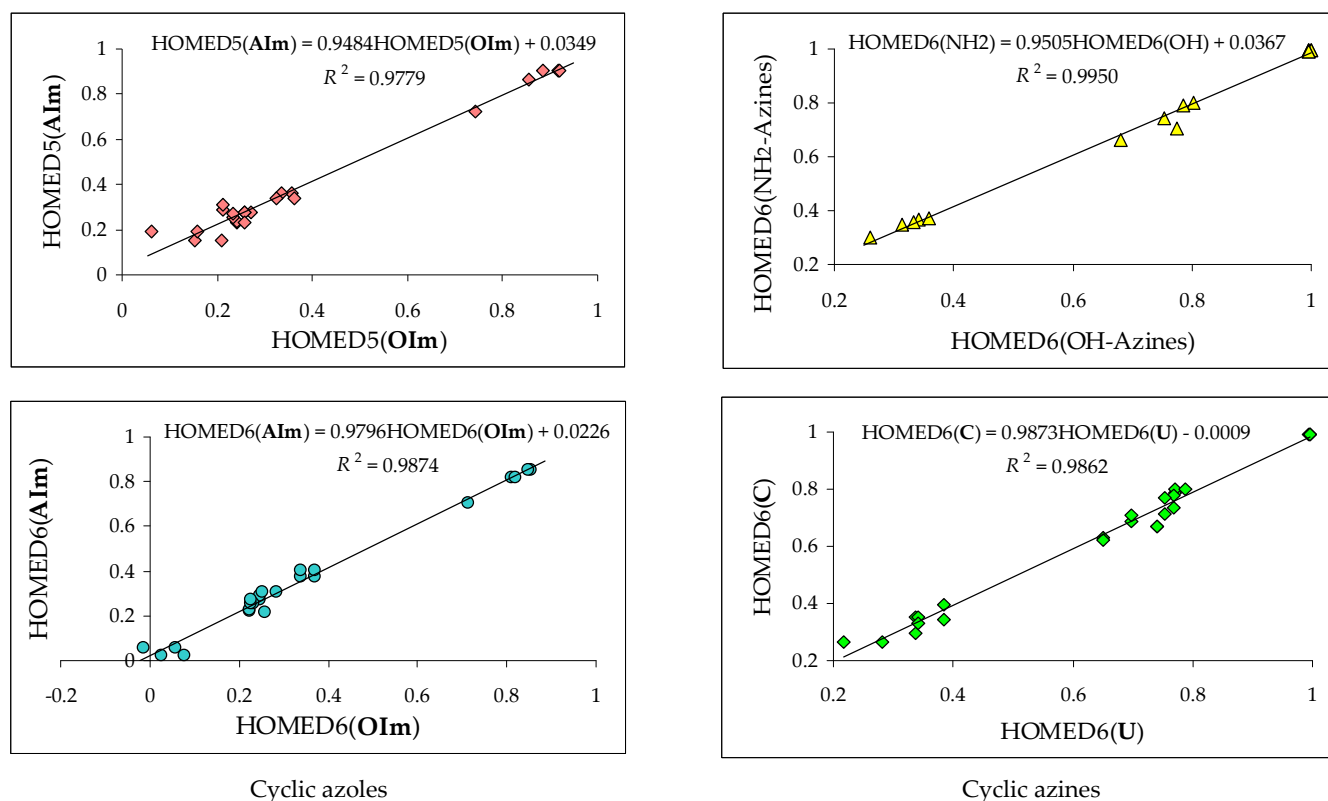


Figure 6. Linear relationships between HOMEDs estimated for tautomers-rotamers of mono-amino (**AIm**) and mono-hydroxy imidazoles (**OIm**), mono-amino and mono-hydroxy substituted cyclic azines, and di-substituted pyrimidine bases (**C**—cytosine and **U**—uracil). HOMED5 and HOMED6 for cyclic azoles correspond to the five-membered ring and the entire molecule, respectively. Data taken from Figures S1–S4 (Supplementary Materials). HOMED6 for cyclic azines, **C**, and **U** refers to the six-membered ring. Data taken from ref. [33,52].

The correlation coefficients ($R \geq 0.98$) and slopes of linear regressions ($a \geq 0.95$) between HOMEDs of **AIm** and **OIm** are close to unity. Slight deviations of some hydroxy and imino isomers (**a** and **b**) from the linear relationships can be a consequence of different favorable and unfavorable interactions between exo- and endo-groups. The change of these interactions when going from **a** to **b** slightly affects electron delocalization and also HOMEDs. Similar linear relationships with analogous correlation coefficients and slopes exist between HOMEDs for isomers of mono-amino and mono-hydroxy azines [33,52], as well as between HOMEDs for isomers of di-substituted pyrimidine nucleic acid bases [33]. These relations between HOMED6s corresponding to the six-membered ring are also included in Figure 6. The HOMED6 data for pyrimidine bases and their model azines were taken from ref. [33]. All these linear relationships between HOMEDs for analogous tautomeric systems containing the five- and six-membered rings quantitatively confirm significant relation between electron delocalization and intramolecular proton transfers.

When HOMEDs for isomers of 1-methyl derivatives (**2A1MIm** and **4O1MIm**) are compared to those of imidazoles (**2AIm** and **4OIm**), interesting effects of the Me group on electron delocalization in the five-membered ring, as well as in the entire delocalized fragment, containing the exo-heterogroup, can be observed. The Me group is not conjugated with the imidazole ring. In the gas phase, it can mainly act by its polarizability and inductive (field) effects. Table 2 summarizes variations in electron delocalization measured by means of the HOMED5 and HOMED6 values when proceeding from the corresponding isomers of **2AIm** to **2A1MIm** and also from isomers of **4OIm** to **4O1MIm**. For tautomers-rotamers without C-sp³ in the five-membered ring, changes of the HOMED values are not very large ($\Delta\text{HOMED} \leq 0.01$). However, stronger Me effects take place for isomers containing the

endo-C-sp³ atom ($\Delta\text{HOMED} > 0.01$). These variations suggest that the Me group affects the bond lengths alternation in the non-aromatic systems with endo-C-sp³ considerably stronger than in already well or moderately delocalized isomers without C-sp³ in the ring.

Table 2. Me effects ^a on the HOMED5 and HOMED6 indices in mono-substituted azoles ^b.

Isomer of X1MIm	Isomers of XIm	Presence of C-sp ³ in the Ring	ΔHOMED5	ΔHOMED6
2A1MIm-6	2AIm-16	no	0.010	0.001
2A1MIm-3a	2AIm-13	no	0.007	0.010
2A1MIm-3b	2AIm-13	no	0.005	0.009
2A1MIm-5a	2AIm-15a	yes	0.025	0.028
2A1MIm-5b	2AIm-15b	yes	0.026	0.030
4O1MIm-6a	4OIm-16a	no	0.004	0.003
4O1MIm-6b	4OIm-16b	no	0.004	0.003
4O1MIm-5	4OIm-15	yes	0.014	0.015

^a Estimated as $\Delta\text{HOMED} = \text{HOMED}(\text{X1MIm}) - \text{HOMED}(\text{XIm})$, where X corresponds to 2-amino (**2A**) or 4-hydroxy (**4O**). HOMEDs taken from Figures S1 and S4 (Supplementary Materials). ^b All isomer abbreviations are in bold like in the text.

The HOMED5 and HOMED7 values estimated for the creatinine isomers and included in Figure S5 (Supplementary Materials) vary in analogous way to that for the model azoles. For the aromatic amino-hydroxy isomers (**Crea-67a** and **Crea-67b**), they are higher than 0.8. For the imino-hydroxy isomers without endo-C-sp³ (**Crea-37aa**, **Crea-37ab**, **Crea-37ba**, and **Crea-37bb**) and zwitterion (**Crea-36**), they are close to 0.7. For isomers containing endo-C-sp³, such as the amino-oxo (**Crea-56**), imino-hydroxy (**Crea-57aa**, **Crea-57ab**, **Crea-57ba**, and **Crea-57bb**), and imino-oxo forms (**Crea-35a** and **Crea-35b**), HOMED5 and HOMED 7 are close to 0.3 and 0.4, respectively.

Analogous differences in electron delocalization were observed previously for the pyrimidine base isocytosine (**iC**), constitutional isomer of cytosine, being a structural part of guanine [34]. Isocytosine (C₄H₅N₃O) contains the two endo-N atoms included in the six-membered ring at 1- and 3-positions and the two exo-heterogroups, NH₂ at 2-position and OH at 4-position, like **Crea**. Among twenty-one isomers possible for **iC**, we selected the fourteen structures (Figure S8, Supplementary Materials) analogous to those of **Crea**-isomers (Figure S5, Supplementary Materials). Their HOMED6 and HOMED8 indices estimated for the six-membered ring and for the entire molecule, respectively, are also included in Figure S8. Although **Crea** (azole with the five-membered ring, seven H atoms, six labile n- electrons, and four labile π -electrons) is structurally different from **iC** (azine with the six-membered ring, five H atoms, four labile n-electrons, and six labile π -electrons), the HOMEDs variations in **Crea**-isomers seem to be parallel to those in the corresponding **iC**-isomers.

Figure 7 illustrates a good linear trend between HOMED5s of **Crea**-isomers and HOMED6s of **iC**-isomers estimated for the five- and six-membered rings, respectively, as well as another linear trend between their HOMEDs7 and HOMED8s estimated for the entire conjugated part, containing the ring and exo-heterogroups. The linear relationships with correlation coefficients *R* higher than 0.98 additionally confirm strong quantitative dependence between electron delocalization and intramolecular proton transfers for analogous tautomeric systems not only between derivatives possessing the six-, or separately, five-membered rings (Figure 6), but also between compounds containing various rings (Figure 7). Note that HOMEDs referring to the tautomer **iC-37** and zwitterion **Crea-36** fit well the linear relationships. The slopes of the regression lines (0.82 and 0.74) are considerably lower than unity, indicating some important differences in electron delocalization in the series of cyclic azole- and azine-isomers.

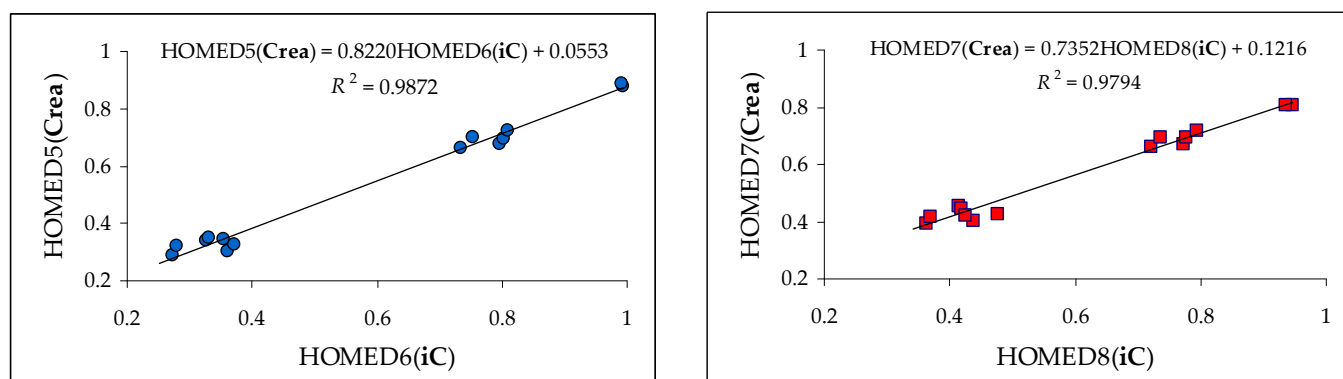


Figure 7. Linear relationships between HOMEDs estimated for **Crea**-isomers and those for the corresponding **iC**-isomers. HOMED5(**Crea**) and HOMED6(**iC**) refer to the five- and six-membered rings. HOMED7(**Crea**) and HOMED8(**iC**) refer to the entire conjugated part containing ring and exo-heterogroups. HOMED data taken from Figures S5 and S8 (Supplementary Materials).

Although variations of electron delocalization are parallel in analogous isomeric mixtures of cyclic azoles and azines, no linear trends exist between their energetic parameters (see in the next section). Consequently, there are no linear trends between the geometric and energetic parameters. This suggests that electron delocalization, being a pivotal factor associated with prototropy, is a less important structural phenomenon in the prediction of the tautomeric preferences for the heterocycles containing the exo NH_2 and OH groups. Analogous schemes of intramolecular proton-transfers and electron delocalization seem to characterize mainly the geometric relations of the tautomeric systems. Aromaticity seems to act as a secondary factor on the composition of tautomeric mixtures.

3.3. Thermochemistry of Isomeric Conversions for Title Compounds

Electron delocalization in the tautomeric systems depends on the number of conjugated sites, the number and type of labile electrons, and the positions of labile protons, whereas tautomeric equilibria and tautomeric preferences depend mainly on acid-base properties of the tautomeric sites. Since electronegativity of C, N, and O atoms significantly differ, acid-base properties of $-\text{CH}_2/= \text{CH}$, $-\text{NH}_2/= \text{NH}$, and $-\text{OH}/= \text{O}$ sites also differ in the cyclic azoles (**2AIm**, **4AIm**, **2OIm**, **4OIm**, **2A1MIm**, **4O1MIm**, and **Crea**) as well as in the cyclic azines including the pyrimidine bases [33,34,52]. Consequently, we do not observe parallel changes between the geometric and energetic parameters for the investigated isomers included in Figures S1–S5 and S8 (Supplementary Materials). When the relative Gibbs energies for the isomers of mono-amino imidazoles (**AIm**) are plotted against those for the isomers of mono-hydroxy imidazoles (**OIm**), and the HOMED7 indices are plotted against the relative Gibbs energies for isomers of **2AIm**, **4AIm**, **2OIm**, and **4OIm**, we obtain scatter plots in all cases (Figure S9 in Supplementary Materials). The same is true when ΔG s of **Crea**-isomers are plotted against ΔG s of **iC**-isomers, and also when HOMEDs of **Crea**-isomers are plotted against their ΔG s (Figure 8). There are no linear trends between the geometric and energetic parameters. This confirms our suggestion that electron delocalization cannot be treated as the main factor that dictates tautomeric preferences in creatinine.

The differences in the acid-base properties of the conjugated tautomeric sites are well described by the relative thermochemical quantities (ΔE , ΔH , and ΔG), equilibrium constants (K), and mole fractions (x_i) [1,2,33,36]. The ΔE , ΔH , $T\Delta S$, ΔG , K , and x_i calculated at the DFT level for all stable isomers of the mono-substituted imidazoles (**2AIm**, **4AIm**, **2OIm**, and **4OIm**), selected 1-methyl derivatives (**2A1MIm** and **4O1MIm**), and creatinine (**Crea**) are listed in Tables S1–S3 (Supplementary Materials). A perusal of these data clearly shows important differences in the tautomeric preferences for the investigated tautomeric compounds (Figure 9). The aromatic forms ($\geq 99.9\%$) predominate only for the mono-amino

model azoles **2AIm**, **4AIm**, and **2A1MIm**. For other derivatives, they belong to minor or rare tautomers. **2OIm** prefers the oxo form **13** without endo-C-sp³ (100%), whereas **4OIm** and **4O1MIm** favor the oxo form **35** (99.8%) and **5** (100%), respectively, with C5-sp³ in the ring. Creatinine containing two exo-heterogroups at the 2- and 4-positions also favors isomers with the endo-C5-sp³ atom, two major imino-oxo isomers **35a** and **35b** (together 97.7%), and the minor amino-oxo form **56** (2.3%). Tautomeric preferences for isocytosine, taken from refs [34,35], are also included in Figure 9 to show the completely different composition of the tautomeric mixture for **iC** (derivative of azine) compared to that for **Crea** (derivative of azole). In the **iC**-mixture, the aromatic amino-hydroxy **78a** (79.67%) and amino-oxo **37** (20.4%) isomers are favored in the gas phase [34]. Isomers of isocytosine containing the endo-C5-sp³ atom belong to the family of exceptionally rare forms.

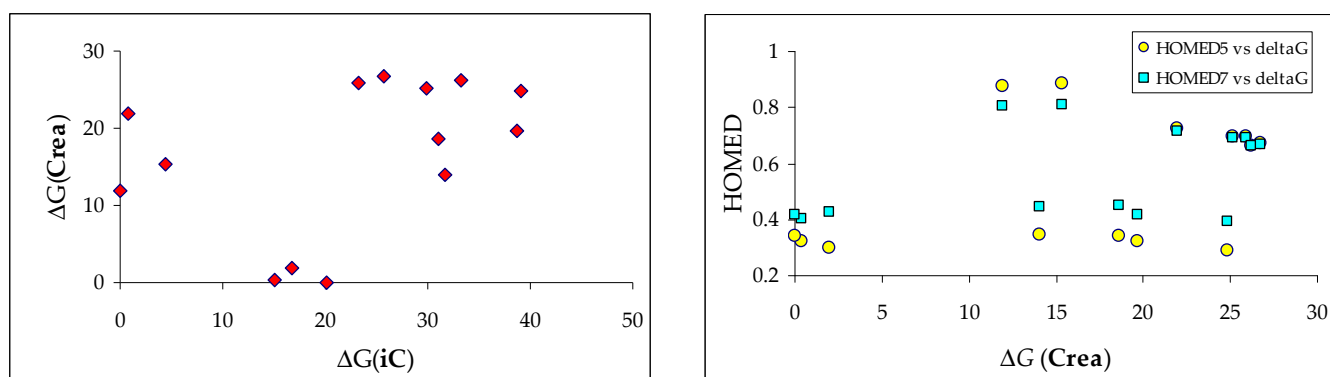


Figure 8. Scatter plots between the relative Gibbs energies (ΔG in kcal mol⁻¹) of all possible **Crea**-isomers and the corresponding **iC**-isomers, and also between HOMEDs and ΔG s of **Crea**-isomers. Data taken from Figures S5 and S8 (Supplementary Materials).

Our DFT results for creatinine can be compared with some scarce literature data. In 1997, Craw et al. published an article [27], in which only two isomers of creatinine (**56** and **35a**) were investigated at various HF, MP2, and DFT levels, and the isomer **35a** was found to be favored in the gas phase. Applying the PCM methods, a change of the tautomeric preference from **35a** in the gas phase to **56** in aqueous solution was documented. Sixteen years later, Gao and coworkers investigated the same isomers of creatinine (**35a** and **56**) in the gas phase (DFT) and aqueous solution (PCM), and they derived an analogous conclusion on the tautomeric-preference change [32]. In 2015, Valadbeigi et al. [13] considered also other tautomers, but not all possible rotamers resulting from conformational and configurational isomerism (see in Table S4, Supplementary Materials). Although calculations have been performed for isolated, micro-, and macro-solvated species at different levels of theory, the results are only partial. Some important isomers have been omitted, for example, the isomer **35b** that is favored in the tautomeric mixture in the gas phase. Only Léon et al. in 2021 published an article [14] in which both experimental and theoretical data for creatinine in various phases have been reported, and they showed that three isomers (**35a**, **35b**, and **56**) can be detected for gaseous creatinine in high-resolution rotational spectra. The relative energies in vacuo have been estimated by quantum-chemical methods for the complete isomeric mixture. Our DFT results are consistent with these literature theoretical data (Table S4, Supplementary Materials).

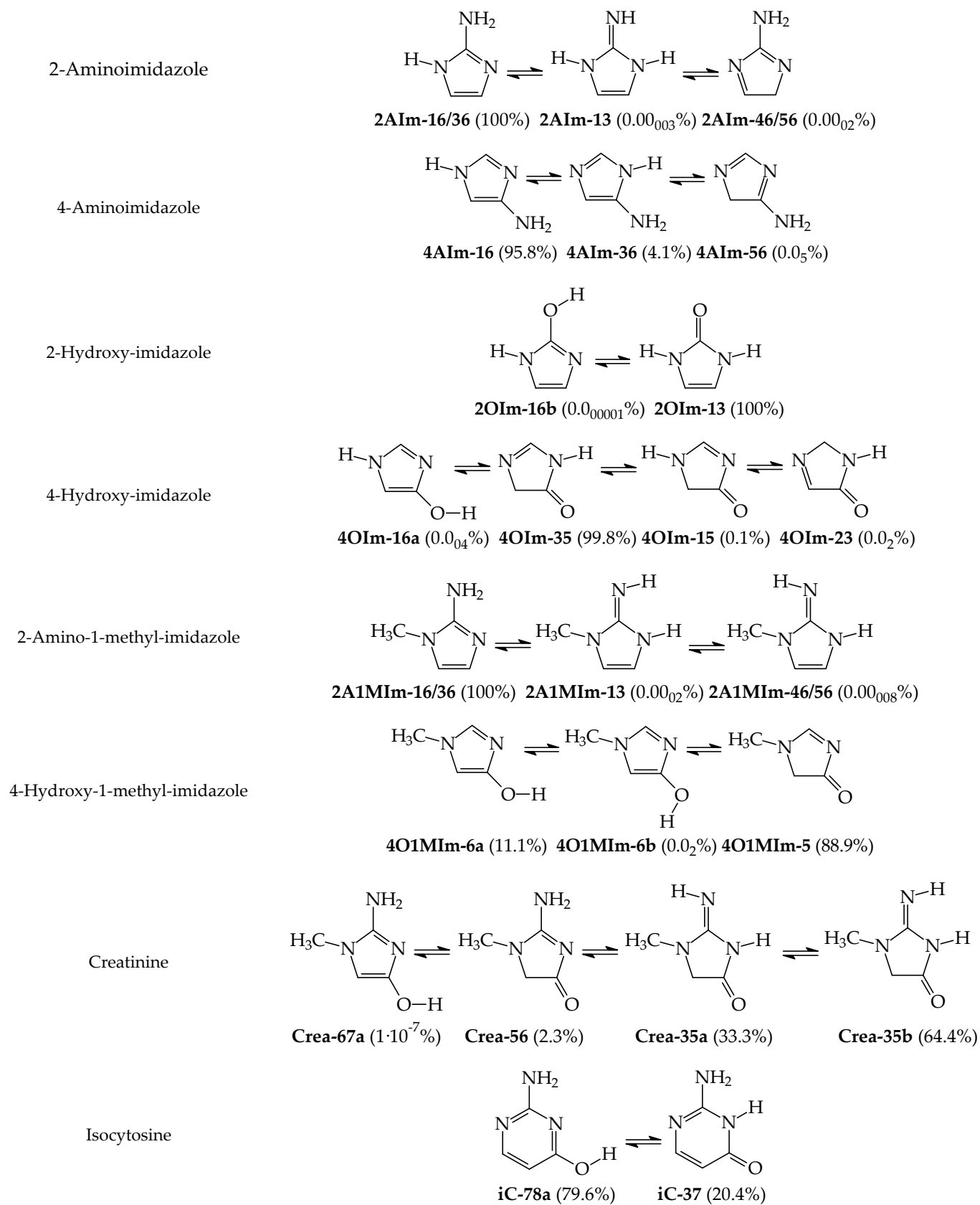


Figure 9. Major, minor, and selected rare tautomers–rotamers for the title compounds and isocytosine. DFT data taken from Tables S1–S3 (Supplementary Materials) and Refs. [33,34].

3.4. Search for Origins of Tautomeric Preferences in Creatinine

Looking for some chemical origins of tautomeric preferences in creatinine, first we confirmed our DFT results for selected keto-enol conversions in 4-hydroxy-imidazole (**4OIm**). Using the G2 and G2(MP2) methods [49,50], we carried out calculations for three isomers of **4OIm** possessing $\Delta G < 6$ kcal mol⁻¹: aromatic hydroxy form **16a**, and two non-aromatic oxo forms containing the C5-sp³ atom in the ring, **15** and **35**. The high level *Gn* theories reproduce sound experimental data for proton-transfer equilibria [33,35,51,52,61–65]. On the basis of our G2 and G2(MP2) thermochemical data compared with those calculated at the DFT level (Table S5, Supplementary Materials), we can see that the differences in the relative energetic parameters calculated at the three levels of theory are very small and close to 1 kcal mol⁻¹. The three methods (DFT, G2, and G2(MP2)) lead to the same conclusion that the non-aromatic tautomer **35** is a favored form in the tautomeric mixture of **4OIm** (99.84, 99.97, and 99.96%, respectively). Stability of the keto form **35** is considerably higher than that of the enol isomer **16a**. These results confirm that the DFT method has been a good choice for investigation of prototropy in azoles. Additionally, our calculations show that aromaticity does not play an important role for tautomeric preference in **4OIm**, contrary to phenol and mono-hydroxy pyridines with the six-membered ring that prefer the aromatic enol forms [33,52]. The energy of aromatic stabilization in **4OIm** is probably lower than that of keto-enol conversion. Moreover, the favored tautomer **35** can be stabilized by favorable intramolecular interactions between C5H₂ and n-electrons of N1, and also between N3H and n-electrons of O6. The other keto form **15** possesses lower stability than the favored isomer **35**, probably because of the intramolecular interactions that are unfavorable in the case of **15**. They correspond to the repulsion of the N1H and C5H₂ groups, and also to the repulsion of the two pairs of n-electrons of N3 and O6.

In the second step, we investigated the effect of the Me group on the tautomeric conversions in 1-methyl derivatives of mono-substituted imidazoles. When going from **2AIm** to **2A1MIm**, the Me effects can be estimated in **2A1MIm** for 1,3-proton shifts from N6 to N3 {amine-imine (amidine) prototropy} and from N3 to C5 (enamine-imine conversion), and also for direct 1,5-proton shift from N6 to C5 (mixture of the two previous prototropic transformations). Analogously, the Me effects can be analyzed in **4O1MIm** for 1,3-proton shift from C5 to O6 (keto-enol rearrangement) when going from **4OIm** to **4O1MIm**. For analysis of these effects, the DFT-calculated relative Gibbs energies can be employed, and the Me effects estimated as differences between ΔG s of the corresponding isomers-pairs of mono-substituted 1-methyl imidazoles **X1MIm** and imidazoles **XIm**, where **X** denotes **2A** or **4O**: $\delta G(\text{Me}) = \Delta G(\text{X1MIm}) - \Delta G(\text{XIm})$. The Me effects, estimated in this way, are summarized in Table 3.

Table 3. Me effects ^a on tautomeric equilibria in mono-substituted azoles ^b.

Pair of Isomers for Proton Transfer		Type of Proton Transfer	$\delta G(\text{Me})$
X1MIm	XIm		
2A1MIm-6 → 2A1MIm-3a	2AIm-16/36 → 2AIm-13	N6→N3	−0.5
2A1MIm-6 → 2A1MIm-3b	2AIm-16/36 → 2AIm-13	N6→N3	−1.1
2A1MIm-3a → 2A1MIm-5a	2AIm-13 → 2AIm-15a/34b	N3→C5	0.7
2A1MIm-3b → 2A1MIm-5b	2AIm-13 → 2AIm-15b/34a	N3→C5	0.3
2A1MIm-6 → 2A1MIm-5a	2AIm-16/36 → 2AIm-15a/34b	N6→C5	0.2
2A1MIm-6 → 2A1MIm-5b	2AIm-16/36 → 2AIm-15b/34a	N6→C5	−0.8
4O1MIm-5 → 4O1MIm-6a	4OIm-15 → 4OIm-16a	C5→O6	−0.8
4O1MIm-5 → 4O1MIm-6b	4OIm-15 → 4OIm-16b	C5→O6	−0.7

^a In kcal mol⁻¹, estimated as $\delta G(\text{Me}) = \Delta G(\text{X1MIm}) - \Delta G(\text{XIm})$, where **X** corresponds to 2-amino (**2A**) or 4-hydroxy (**4O**). ΔG taken from Figures S1 and S4 (Supplementary Materials). ^b All isomer abbreviations are in bold like in the text.

The Me effects are not very strong, and they slightly depend on the configuration about =N6H in the 2-imino forms of imidazoles and on conformation about −O6H in 4-hydroxy

imidazoles. Generally, the Me group, structurally introduced at N1 in **X1MIm**, slightly influences the relative Gibbs energies for the considered intramolecular proton transfers by 0.2–1.1 kcal mol^{−1}. So small variations indicate that the Me effects cannot dictate particular stability of the amino-oxo (**56**) and imino-oxo forms (**35a** and **35b**) for **Crea**. Note that the estimated $\delta G(\text{Me})$ values are negative or positive. They correspond to the ΔG decrease or increase between the selected pair of isomers, showing some favored or unfavored Me effects on the selected proton-transfer. The Me group slightly favors the 1,3-proton shift from N6 to N3 in **2A1MIm**, in a slightly higher degree for the configuration **b** than **a**. It also favors the 1,5-proton shift from N6 to C5 for the same configuration **b**. In the case of **4O1MIm**, only one type of proton-transfer (keto-enol) from C5 to O6 could be analyzed and Me effects estimated. For the two $-\text{O6H}$ conformations **a** and **b**, ΔG s are lower for the Me-derivative **4O1MIm** than for **4OIm**, indicating that enolization is slightly favored for **4O1MIm** in comparison to **4OIm**.

Additionally, we analyzed the effects of the intramolecular interactions between the exo- and endo-functional groups (less or more favorable and less or more unfavorable) resulting from the rotational isomerism about $-\text{OH}$ and the geometrical isomerism about $=\text{NH}$, when proceeding from the isomer **a** to isomer **b**. For isomers with less or more favorable intramolecular interactions between the exo- and endo-groups, the relative Gibbs energies are lower than for those with less or more unfavorable ones (see in Figures S1–S5 and S8, Supplementary Materials). Difference between the relative Gibbs energies of the isomers **a** and **b** can be considered as the measure of difference in the intramolecular interactions $\{\delta G(=\text{NH})$ or $\delta G(-\text{OH}) = \Delta G(\text{isomer a}) - \Delta G(\text{isomer b})\}$. In Table 4, the effects of $\delta G(=\text{NH})$ and $\delta G(-\text{OH})$, estimated in this way for isomers of mono-substituted imidazoles (**2AIm**, **2A1MIm**, **4AIm**, **2OIm**, **4OIm**, and **4O1MIm**) and creatinine (**Crea**), are compared with those for the corresponding isomers of isocytosine (**iC**).

Table 4. Effects of intramolecular interactions^a between the exo- and endo-groups on the stability of the isomers **a** and **b** in mono-substituted azoles and di-substituted creatinine compared to those in isocytosine^b.

Pair of Isomers a and b	$\delta G(=\text{NH})$	Pair of Isomers a and b	$\delta G(-\text{OH})$
2AIm-15a/34b → 2AIm-15b/34a	−3.9	2OIm-46a/56b → 2OIm-46b/56a	−0.8
2A1MIm-3a → 2A1MIm-3b	−0.6	4OIm-16a → 4OIm-16b	3.8
2A1MIm-5a → 2A1MIm-5b	−4.9	4OIm-26a → 4OIm-26b	4.8
4AIm-23a → 4AIm-23b	−0.6	4OIm-46a → 4OIm-46b	0.6
4AIm-15a → 4AIm-15b	4.4	4OIm-56a → 4OIm-56b	5.1
4AIm-35a → 4AIm-35b	−1.6	4O1MIm-6a → 4O1MIm-6b	3.9
Crea-37aa → Crea-37ba	−0.5	Crea-67a → Crea67b	3.5
Crea-37ab → Crea-37bb	−0.7	Crea-37aa → Crea-37ab	−0.8
Crea-57aa → Crea-57ba	−4.5	Crea-37ba → Crea-37bb	−1.1
Crea-57ab → Crea-57bb	−5.2	Crea-57aa → Crea-57ab	6.3
Crea-35a → Crea-35b	−0.4	Crea-57ba → Crea-57bb	5.6
iC-38aa → iC-38ba	7.5	iC-78a → iC-78b	4.4
iC-38ab → iC-38bb	6.6	iC-38aa → iC-38ab	−2.4
iC-58aa → iC-58ba	0.6	iC-38ba → iC-38bb	−3.3
iC-58ab → iC-58bb	−0.4	iC-58aa → iC-58ab	8.0
iC-35a → iC-35b	5.1	iC-58ba → iC-58bb	7.0

^a In kcal mol^{−1}, estimated as $\delta G(=\text{NH})$ or $\delta G(-\text{OH}) = \Delta G(\text{isomer a}) - \Delta G(\text{isomer b})$, ΔG taken from Figures S1–S5 and S8 (Supplementary Materials). ^b All isomer abbreviations are in bold like in the text.

The comparison indicates that some absolute δG values referring to changes in the intramolecular interactions for the isomers **a** and **b** in the mono-substituted azoles (**2AIm**, **2A1MIm**, **4AIm**, **2OIm**, **4OIm**, and **4O1MIm**) are considerably higher than the Me effects in **2A1MIm** and **4O1MIm** (Table 3). The strongest effects (3.8–5.1 kcal mol^{−1}) take place for the tautomers, for which favorable interactions in **a** change into unfavorable interactions in **b** and vice versa. When interactions in both isomers (**a** and **b**) are unfavorable or favorable, the absolute δG values vary from 0.6 to 1.6 kcal mol^{−1}. Analogous effects are observed for **Crea**- and **iC**-isomers, for which the absolute δG values vary from 0.4–1.1 to 3.5–6.3

and from 0.4–3.3 to 4.4–8.0 kcal mol⁻¹, respectively. Although favorable intramolecular interactions between the functional exo- and endo-groups influence the stability of particular isomers (**a** or **b**) and reduce the relative Gibbs energies, these interactions can be considered as secondary factors that only change isomer-orders. In the case of **Crea**-isomers, they have slight effects on the energetic-order of the favored imino-isomers **35a** and **35b** (−0.4 kcal mol⁻¹), because similar intramolecular interactions operate in the two isomers between the exo =NH and endo NCH₃ and NH groups. A different situation takes place for the aromatic amino-hydroxy **iC**-isomers (**78a** and **78b**), for which the difference between the favorable interactions in **78a** and the unfavorable interactions in **78b** considerably reduces the Gibbs energy of **78a** (by 4.4 kcal mol⁻¹) that it predominates in the **iC**-isomeric mixture [34].

Finally, in the last step, we analyzed the effects of the additional functional group on the amine-imine (amidine), enamine-imine, and keto-enol conversions when proceeding from a pair of **X1MIm**-isomers to the corresponding pair of **Crea**-isomers. The two heteroatomic groups (NH₂ and OH) belong to the family of electron-donating substituents. In the gas phase, they act by the sum of their polarizability, field-inductive, and resonance effects. Additionally, they can interact (favorable or unfavorable) with the endo neighboring groups. Hence, the total effects of the additionally introduced exo-group can strongly influence the proton-transfer for the group already present in the molecule. For the estimation of these effects, the relative Gibbs energies can be used for the corresponding proton-transfers, and the effects of 2-NH₂ and 4-OH can be calculated as differences between ΔG s of the corresponding pairs of **Crea**-isomers and **X1MIm**-isomers: $\delta G(2\text{-NH}_2)$ or $\delta G(4\text{-OH}) = \Delta G(\text{Crea}) - \Delta G(\text{X1MIm})$. The calculated $\delta G(2\text{-NH}_2)$ and $\delta G(4\text{-OH})$ values are given in Table 5.

Table 5. Effects of exo-heterogroups (2-NH₂ and 4-OH)^a on tautomeric equilibria for creatinine^b.

Pair of Isomers for Proton Transfer		Proton Transfer	$\delta G(4\text{-OH})$	$\delta G(2\text{-NH}_2)$
Crea	2A1MIm			
Crea-67a → Crea-37aa	2A1MIm-6 → 2A1MIm-3a	N6→N3	6.47 (a)	
Crea-67a → Crea-37ba	2A1MIm-6 → 2A1MIm-3b	N6→N3	6.56 (a)	
Crea-67b → Crea-37ab	2A1MIm-6 → 2A1MIm-3a	N6→N3	2.17 (b)	
Crea-67b → Crea-37bb	2A1MIm-6 → 2A1MIm-3b	N6→N3	2.04 (b)	
Crea-37a → Crea-57aa	2A1MIm-3a → 2A1MIm-5a	N3→C5	−16.67 (a)	
Crea-37a → Crea-57ba	2A1MIm-3b → 2A1MIm-5b	N3→C5	−16.39 (a)	
Crea-37b → Crea-57ab	2A1MIm-3a → 2A1MIm-5a	N3→C5	−9.53 (b)	
Crea-37b → Crea-57bb	2A1MIm-3b → 2A1MIm-5b	N3→C5	−9.69 (b)	
Crea-67a → Crea-57aa	2A1MIm-6 → 2A1MIm-5a	N6→C5	−10.20 (a)	
Crea-67a → Crea-57ba	2A1MIm-6 → 2A1MIm-5b	N6→C5	−9.83 (a)	
Crea-67b → Crea-57ab	2A1MIm-6 → 2A1MIm-5a	N6→C5	−7.36 (b)	
Crea-67b → Crea-57bb	2A1MIm-6 → 2A1MIm-5b	N6→C5	−7.65 (b)	
Crea-67a → Crea-56	4O1MIm-6a → 4O1MIm-5	O6→C5		−8.69
Crea-67b → Crea-56	4O1MIm-6b → 4O1MIm-5	O6→C5		−8.21

^a In kcal mol⁻¹, estimated as $\delta G(2\text{-NH}_2) = \Delta G(\text{Crea}) - \Delta G(\text{2A1MIm})$, $\delta G(4\text{-OH}) = \Delta G(\text{Crea}) - \Delta G(\text{4O1MIm})$. ΔG taken from Figures S1, S4, and S5 (Supplementary Materials). ^b All isomer abbreviations are in bold like in the text.

Interestingly, the total internal effects of the exo-heterogroups are very strong and can be responsible for the change of the tautomeric preferences in **Crea**. Although the additional exo −OH group, structurally linked to C4 in **2A1MIm**, increases ΔG s for proton transfer from N6 to N3 in **Crea** by ca. 2 kcal mol⁻¹ for conformation **b** and by 6–7 kcal mol⁻¹ for conformation **a**, the successive proton-transfer from N3 to C5 is so favorable in **Crea** in comparison to **2A1MIm** that ΔG s are strongly reduced by 9–10 kcal mol⁻¹ for conformation **b**, and even by 16–17 kcal mol⁻¹ for conformation **a**. Consequently, direct proton transfer from N6 to C5 is also strongly favored in **Crea**. The ΔG values decrease by 7–8 kcal mol⁻¹ for conformation **b** and by ca. 10 kcal mol⁻¹ for conformation **a**. The additional exo NH₂ group, structurally introduced in **4O1MIm** at 2-position, also reduces ΔG s for proton transfer from O6 to C5 in **Crea** when compared to those in **4O1MIm** by 8–9 kcal mol⁻¹.

The high ΔG s-reduction effects of the additional exo-groups indicate that they can be the main factors that influence tautomeric preferences in **Crea**.

4. Conclusions

The application of the same level of theory for investigation of the complete tautomeric, conformational, and configurational transformations in creatinine and model azoles gave us the possibility to find some origins for exceptional tautomeric preferences in creatinine, and also to explain why the non-aromatic amino-oxo (**Crea-56**) and imino-oxo tautomers (**Crea-35**) are more stable in the gas phase than the aromatic amino-hydroxy form (**Crea-67**). On the basis of our DFT data for creatinine and model azoles, compared to those previously reported for the complete isomeric conversions in pyrimidine nucleic acid bases and their model azines [33,52], we can derive the following conclusions.

Aromaticity is not the main factor that influences the tautomeric preference in creatinine containing the five-membered ring, contrary to isocytosine possessing the six-membered ring [34,35]. Nevertheless, variations of electron delocalization in isomers of the two molecules, having the tautomeric sites at analogous positions, are parallel. The aromatic isomers with the labile protons at the exo-groups are well delocalized and their HOMED indices (measure of electron delocalization) are larger than 0.8. The imino-oxo isomers without endo-C-sp³ are moderately delocalized and their HOMED indices are between 0.7 and 0.8, and those with C-sp³ in the ring are weakly delocalized and their HOMED indices are lower than 0.5. Good linear relationships exist between the HOMED indices for isomers of creatinine and isocytosine (Figure 7). However, variations of electron delocalization (HOMEDs) are not parallel to those of isomeric stability (measured by ΔG s), because of the lack of linear trends between energetic parameters (ΔG s) of their isomers (Figure 8).

Only detailed analyses of various internal effects in investigated derivatives such as the electronic effects of the exo-groups (Me, NH₂, and OH) and the intramolecular interactions between the exo- and endo-heterogroups made it possible to select the most important factors that decide about the tautomeric preferences in creatinine. We found that the Me group at N1 has a small effect on the tautomeric conversion { $\delta G(\text{Me})$ not higher than 1 kcal mol⁻¹, see in Table 3}. The effects of favorable intramolecular interactions between exo- and endo-heterogroups are slightly stronger, and in some cases, the relative Gibbs energies change even by 5–6 kcal mol⁻¹ (Table 4). The intramolecular interactions affect mainly relative stabilities of the isomers **a** and **b**. They only slightly influence tautomeric preferences in creatinine { $\delta G(=\text{NH}) < 1$ kcal mol⁻¹ for pair of the favored imino-oxo isomers **Crea-35a** and **Crea-35b**}.

The most important internal effects that strongly change the relative Gibbs energies result from the presence of additional exo-group in creatinine when compared with model mono-substituted 1-methyl imidazoles **2A1MIm** and **4O1MIm** (Table 5). Figure 10 summarizes the selected effects of the additional exo-heterogroup. The NH₂ group introduced at 2-position in **Crea** strongly favors the proton-transfer from O7 to C5 when compared to the analogous one in **4O1MIm**, and its total effect can explain significant participation of the amino-oxo tautomer (**56**) in the tautomeric mixture of creatinine. On the other hand, the introduction of the more stable keto form in **2A1MIm** favors proton transfer from N6 to N3 and can explain the high stability of the imino-oxo isomers (**35a** and **35b**). These energetic effects in derivatives with the five-membered ring are completely different from those in isocytosine with the six-membered ring, for which isomers with endo-C-sp³ are exceptionally rare forms and the aromatic amino-hydroxy form **iC-78a** is favored [34,35].

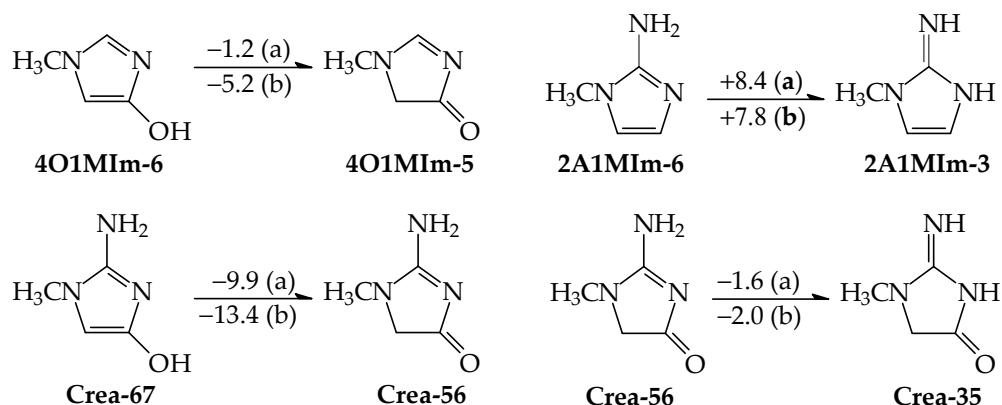


Figure 10. Selected effects (ΔG s in kcal mol^{-1}) of additional exo-groups on prototropic conversions when proceeding from model 1-methyl imidazoles to creatinine.

Supplementary Materials: The following supporting information can be downloaded at: <https://www.mdpi.com/article/10.3390/sym16010098/s1>, Structures, HOMEDs, and ΔG s for tautomers-rotamers of **2AIm** and **2A1MIm** (Figure S1), **4AIm** (Figure S2), **2OIm** (Figure S3), **4OIm** and **4O1MIm** (Figure S4), **Crea** (Figure S5) and **iC** (Figure S8); Linear trends between HOMED5s (Figure S6) and HOMED6s (Figure S7) for isomers of **AIm** and **OIm**; Plots between ΔG s of **AIm** and **OIm** and between their HOMEDs and ΔG s (Figure S9); Thermochemical parameters for isomers of **AIm** and **OIm** (Table S1), **A1MIm** and **O1MIm** (Table S2) and **Crea** (Table S3); Comparison of DFT results with the literature data for **Crea**-isomers (Table S4); Comparison of DFT, G2 and G2(MP2) results for selected **4OIm**-isomers (Table S5).

Funding: This work received no external funding.

Data Availability Statement: Data are contained within the article and Supplementary Materials.

Acknowledgments: Author thanks the Warsaw University of Life Sciences (SGGW) for providing support.

Conflicts of Interest: The author declares no conflicts of interest.

References

- Elguero, J.; Katritzky, A.R.; Denisko, O.V. Prototropic Tautomerism of Heterocycles: Heteroaromatic Tautomerism—General Overview and Methodology. *Adv. Heterocycl. Chem.* **2000**, *76*, 184.
- Raczyńska, E.D.; Kosińska, W.; Ośmiałowski, B.; Gawinecki, R. Tautomeric Equilibria in Relation to π -Electron Delocalization. *Chem. Rev.* **2005**, *105*, 3561–3612. [[CrossRef](#)] [[PubMed](#)]
- Minkin, V.I.; Garnovskii, A.D.; Elguero, J.; Katritzky, A.R.; Denisko, O.V. The Tautomerism of Heterocycles: Five-Membered Rings with Two or More Heteroatoms. *Adv. Heterocycl. Chem.* **2006**, *76*, 157–323.
- Stanovnik, B.; Tišler, M.; Katritzky, A.R.; Denisko, O.V. The Tautomerism of Heterocycles: Substituent Tautomerism of Six-Membered Ring Heterocycles. *Adv. Heterocycl. Chem.* **2006**, *91*, 1–134.
- Lempert, C. The Chemistry of the Glycoyamidines. *Chem. Rev.* **1959**, *59*, 667–736. [[CrossRef](#)]
- Matsumoto, K.; Rapoport, H. Preparation and Properties of Some Acyl-Guanidines. *J. Org. Chem.* **1968**, *33*, 552–558. [[CrossRef](#)]
- Hunter, A. *Creatine and Creatinine*; Monographs on Biochemistry, Longmans, Green & Co.: London, UK, 1928.
- Cannan, R.K.; Shore, A. The Creatine-Creatinine Equilibrium. The Apparent Dissociation Constants of Creatine and Creatinine. *Biochem. J.* **1928**, *22*, 920–929. [[CrossRef](#)]
- Taylor, E.H. *Clinical Chemistry*; John Wiley and Sons: New York, NY, USA, 1989; pp. 58–62.
- Gangopadhyay, D.; Sharma, P.; Singh, S.K.; Deckert, V.; Popp, J.; Singh, R.K. Surface Enhanced Raman Scattering Based Reaction Monitoring of in vitro Decyclization of Creatinine \rightarrow Creatine. *RSC Adv.* **2016**, *6*, 58943–58949. [[CrossRef](#)]
- Kenyon, G.L.; Rowley, G.L. Tautomeric Preferences among Glycoyamidines. *J. Am. Chem. Soc.* **1971**, *93*, 5552–5560. [[CrossRef](#)]
- Das, G. Rotational Aspects of Non-Ionized creatine in the Gas Phase. *Monatsh. Chem.* **2014**, *145*, 1431–1441. [[CrossRef](#)]
- Valadbeigi, Y.; Ilbeigi, V.; Tabrizchi, M. Effect of Mono- and Di-hydration on the Stability and Tautomerisms of Different Tautomers of Creatinine: A Thermodynamic and Mechanistic Study. *Comput. Theor. Chem.* **2015**, *1061*, 27–35. [[CrossRef](#)]
- Léon, I.; Tasinato, N.; Spada, L.; Alonso, E.R.; Mata, S.; Balbi, A.; Puzzarini, C.; Alonso, J.L.; Barone, V. Looking for the Elusive Imine Tautomer of Creatinine: Different States of Aggregation Studied by Quantum Chemistry and Molecular Spectroscopy. *ChemPlusChem* **2021**, *86*, 1374–1386. [[CrossRef](#)] [[PubMed](#)]

15. Wyss, M.; Kaddurah-Daouk, R. Creatine and Creatinine Metabolism. *Physiol. Rev.* **2000**, *80*, 1107–1213. [[CrossRef](#)]
16. Narimani, R.; Esmaeili, M.; Rasta, S.H.; Khosroshahi, H.T.; Mobed, A. Trend in Creatinine Determining Methods: Conventional Methods to Molecular-Based Methods. *Anal. Sci. Adv.* **2021**, *2*, 308–325. [[CrossRef](#)]
17. Finlay, M.R. Quackery and Cookery: Justus von Liebig's Extract of Meat and the Theory of Nutrition in the Victorian Age. *Bull. Hist. Med.* **1992**, *66*, 404–418. [[PubMed](#)]
18. du Pré, S.; Mendel, H. The Crystal Structure of Creatinine. *Acta Cryst.* **1955**, *8*, 311–313. [[CrossRef](#)]
19. Grzybowski, A.K.; Datta, S.P. The Ionisation Constant of the Protonated Form of Creatinine. *J. Chem. Soc.* **1964**, 187–196. [[CrossRef](#)]
20. Srinivasan, R.; Stewart, R. The Catalysis of Proton Exchange in Creatinine by General Acids and General Bases. *Can. J. Chem.* **1975**, *53*, 224–231. [[CrossRef](#)]
21. Dietrich, R.F.; Marletta, M.A.; Kenyon, G.L. Carbon-13 Nuclear Magnetic Resonance Studies of Creatine, Creatinine and Some of their analogs. *Org. Magn. Reson.* **1980**, *13*, 79–88. [[CrossRef](#)]
22. Butler, A.R.; Glidewell, C. Creatinine: An Examination of Its Structure and Some of Its Reactions by Synergistic Use of MNDO Calculations and Nuclear Magnetic Resonance Spectroscopy. *J. Chem. Soc. Perkin Trans. 2* **1985**, *9*, 1465–1467. [[CrossRef](#)]
23. Reddick, R.E.; Kenyon, G.L. Syntheses and NMR Studies of Specifically Labeled [2-15N]Phosphocreatine, [2-15N]Creatinine, and Related 15N-Labeled Compounds. *J. Am. Chem. Soc.* **1987**, *109*, 4380–4387. [[CrossRef](#)]
24. Trendafilova, N.; Kurbakova, A.P.; Efimenko, I.A.; Mitewa, M.; Bontchev, P.R. Infrared Spectra of Pt(II) Creatinine Complexes. Normal Coordinate Analysis of Creatinine and Pt(Creat)₂(NO₂)₂. *Spectrochim. Acta Part A* **1991**, *47*, 577–584. [[CrossRef](#)]
25. Arakali, A.V.; McCloskey, J.; Parthasarathy, R.; Alderfer, J.L.; Chheda, G.B.; Srikrishnan, T. Study of Creatinine and Its 5-Alkoxy Analogs: Structure and Conformational Studies in the Solid and Solution States by X-Ray Crystallography, NMR, UV and Mass Spectrometry. *Nucleosides Nucleotides Nucleic Acids* **1997**, *16*, 2193–2218. [[CrossRef](#)]
26. Bell, T.W.; Hou, Z.; Luo, Y.; Drew, M.G.B.; Chapoteau, E.; Czech, B.P.; Kumar, A. Detection of Creatinine by a Designed Receptor. *Science* **1995**, *269*, 671–674. [[CrossRef](#)] [[PubMed](#)]
27. Craw, J.S.; Greatbanks, S.B.; Hillier, I.H.; Harrison, M.J.; Burton, N.A. Solvation and Solid State Effects on the Structure of the Tautomers of Creatinine. *J. Chem. Phys.* **1997**, *106*, 6612–6617. [[CrossRef](#)]
28. Craw, S.J.; Hillier, I.H.; Morris, G.A.; Vincent, M.A. Theoretical and Experimental Studies of the Barrier to Amine Rotation in Creatinine: Influence of Solvation Models and Explicit Solvation. *Mol. Phys.* **1997**, *92*, 421–428. [[CrossRef](#)]
29. Kotsyubynskyy, D.; Molchanov, S.; Gryff-Keller, A. Creatinine and Creatinium Cation in DMSO-d₆ Solution. Structure and Restricted Internal Rotation of NH₂ Group. *Magn. Res. Chem.* **2004**, *42*, 1027–1036. [[CrossRef](#)] [[PubMed](#)]
30. Bayrak, C.; Bayari, S.H. Vibrational and DFT Studies of Creatinine and Its Metal Complexes. *Hacet. J. Biol. Chem.* **2010**, *38*, 107–118.
31. Vikram, K.; Mishra, S.; Srivastava, S.K.; Singh, R.K. Low Temperature Raman and DFT Study of Creatinine. *J. Mol. Struct.* **2012**, *1012*, 141–150. [[CrossRef](#)]
32. Gao, J.; Hu, Y.; Li, S.; Zhang, Y.; Chen, X. Tautomeric Equilibrium of Creatinine and Creatinium Cation in Aqueous Solution Explored by Raman Spectroscopy and Density Functional Theory Calculations. *Chem. Phys.* **2013**, *410*, 81–89. [[CrossRef](#)]
33. Raczyńska, E.D. On Prototropy and Bond Length Alternation in Neutral and Ionized Pyrimidine Bases and Their Model Azines in Vacuo. *Molecules* **2023**, *28*, 7282. [[CrossRef](#)] [[PubMed](#)]
34. Raczyńska, E.D. Quantum-Chemical Studies on the Favored and Rare Isomers of Isocytosine. *Comput. Theor. Chem.* **2017**, *1121*, 58–67. [[CrossRef](#)]
35. Raczyńska, E.D.; Makowski, M. Effects of Positive and Negative Ionization on Prototropy in Pyrimidine Bases: An Unusual Case of Isocytosine. *J. Phys. Chem. A* **2018**, *122*, 7863–7879. [[CrossRef](#)] [[PubMed](#)]
36. Elguero, J.; Marzin, C.; Katritzky, A.R.; Linda, P. *The Tautomerism of Heterocycles*; Academic Press: Cambridge, MA, USA, 1976; pp. 1–655.
37. Ögretir, C.; Yarligan, S. AM1, PM3 and MNDO Study of the Tautomerism of 2-, 4- or 5-Imidazolones and Their Thio- and Azo-Analogs. *J. Mol. Struct. (Theochem)* **1996**, *366*, 227–231. [[CrossRef](#)]
38. Kurzepa, M.; Dobrowolski, J.C.; Mazurek, A.P. Theoretical Studies on Tautomerism and IR Spectra of C-5 Substituted Imidazoles. *J. Mol. Struct.* **2001**, *565–566*, 107–113. [[CrossRef](#)]
39. Zhang, H.; Xue, Y.; Xie, D.-Q.; Yan, G.-S. Ab initio Calculation and Monte Carlo Simulation on Tautomerism and Proton Transfer of 2-Hydroxyimidazole in Gas Phase and Water. *Acta Chim. Sin.* **2005**, *63*, 791–796.
40. Raczyńska, E.D. Application of the Extended HOMED (Harmonic Oscillator Model of Aromaticity) Index to Simple and Tautomeric Five-Membered Heteroaromatic Cycles with C, N, O, P, and S Atoms. *Symmetry* **2019**, *11*, 146. [[CrossRef](#)]
41. Parr, R.G.; Yang, W. *Density Functional Theory of Atoms and Molecular Orbital Theory*; Oxford University Press: New York, NY, USA, 1989.
42. Becke, A.D. Density-Functional Thermochemistry. III. The Role of Exact Exchange. *J. Chem. Phys.* **1993**, *98*, 5648–5652. [[CrossRef](#)]
43. Lee, C.; Yang, W.; Parr, R.G. Development of the Colle-Salvetti Correlation-Energy Formula into a Functional of the Electron Density. *Phys. Rev. B* **1988**, *37*, 785–789. [[CrossRef](#)]
44. Hehre, W.J.; Radom, L.; Schleyer, P.v.R.; Pople, J.A. *Ab Initio Molecular Theory*; Wiley: New York, NY, USA, 1986.
45. Raczyńska, E.D.; Makowski, M.; Hallmann, M.; Kamińska, B. Geometric and Energetic Consequences of Prototropy for Adenine and Its Structural Models—A Review. *RSC Adv.* **2005**, *5*, 36587. [[CrossRef](#)]

46. Maksić, Z.B.; Kovačević, B.; Vianello, R. Advances in determining the absolute proton affinities of neutral organic molecules in the gas phase and their interpretation: A theoretical account. *Chem. Rev.* **2012**, *112*, 5240–5270. [[CrossRef](#)] [[PubMed](#)]
47. Leito, I.; Koppel, I.A.; Koppel, I.; Kaupmees, K.; Tshepelevitsh, S.; Saame, J. Basicity limits of neutral organic superbases. *Angew. Chem. Int. Ed.* **2015**, *54*, 9262–9265. [[CrossRef](#)] [[PubMed](#)]
48. Raczyńska, E.D.; Kamińska, B. Structural and Thermochemical Consequences of Prototropy and Ionization for the Biomolecule Xanthine in Vacuo. *J. Chem. Thermodyn.* **2022**, *171*, 106788. [[CrossRef](#)]
49. Curtiss, L.A.; Raghavachari, K.; Trucks, G.W.; Pople, J.A. Gaussian-2 Theory for Molecular Energies of First- and Second-Row Compounds. *J. Chem. Phys.* **1991**, *94*, 7221–7230. [[CrossRef](#)]
50. Curtiss, L.A.; Raghavachari, K.; Pople, J.A. Gaussian-2 Theory Using Reduced Møller-Plesset Orders. *J. Chem. Phys.* **1993**, *98*, 1293–1298. [[CrossRef](#)]
51. Smith, B.J.; Radom, L. Assigning Absolute Values to Proton Affinities: A Differentiation Between Competing Scales. *J. Am. Chem. Soc.* **1993**, *115*, 4885–4888. [[CrossRef](#)]
52. Raczyńska, E.D. Electron Delocalization and Relative Stabilities for the Favored and Rare Tautomers of Hydroxyazines in the Gas Phase—A Comparison with Aminoazines. *Comput. Theor. Chem.* **2014**, *1042*, 8–15. [[CrossRef](#)]
53. Frisch, M.J.; Trucks, G.W.; Schlegel, H.B.; Scuseria, G.E.; Robb, M.A.; Cheeseman, J.R.; Montgomery, J.A., Jr.; Vreven, T.; Kudin, K.N.; Burant, J.C.; et al. *Gaussian-03, Revision E.01*; Gaussian, Inc.: Wallingford, CT, USA, 2004.
54. Kruszewski, J.; Krygowski, T.M. Definition of Aromaticity Basing on the Harmonic Oscillator Model. *Tetrahedron Lett.* **1972**, *13*, 3839–3842. [[CrossRef](#)]
55. Krygowski, T.M.; Kruszewski, J. Aromaticity of Thiophene, Pyrrole and Furan in Terms of Aromaticity Indices and Hammett σ Constants. *Bull. Acad. Pol. Sci. Chim.* **1974**, *22*, 871–876.
56. Krygowski, T.M. Crystallographic Studies of Inter- and Intramolecular Interactions Reflected in Aromatic Character of π -Electron Systems. *J. Chem. Inform. Comput. Sci.* **1993**, *33*, 70–78. [[CrossRef](#)]
57. Perrin, C.L.; Agranat, I.; Bagno, A.; Braslavsky, S.E.; Fernandes, P.A.; Gal, J.-F.; Lloyd-Jones, G.C.; Mayr, H.; Murdoch, J.R.; Nudelman, N.S.; et al. Glossary of Terms Used in Physical Organic Chemistry (IUPAC Recommendations 2021). *Pure Appl. Chem.* **2022**, *94*, 353–534. [[CrossRef](#)]
58. Raczyńska, E.D.; Makowski, M.; Zientara-Rytter, K.; Kolczyńska, K.; Stępniewski, T.M.; Hallmann, M. Quantum-Chemical Studies on the Favored and Rare Tautomers of Neutral and Redox Adenine. *J. Phys. Chem. A* **2013**, *117*, 1548–1559. [[CrossRef](#)] [[PubMed](#)]
59. Alkorta, I.; Elguero, J.; Liebman, J.F. The annular tautomerism of imidazoles and pyrazoles: The possible existence of nonaromatic forms. *Struct. Chem.* **2006**, *17*, 439–444. [[CrossRef](#)]
60. Raczyńska, E.D. Quantum-chemical studies of the consequences of one-electron oxidation and one-electron reduction for imidazole in the gas phase and water. *Comput. Theor. Chem.* **2012**, *993*, 73–79. [[CrossRef](#)]
61. Smith, B.J.; Radom, L. Calculating of Proton Affinities Using the G2(MP2,SVP) Procedure. *J. Phys. Chem.* **1995**, *99*, 6468–6471. [[CrossRef](#)]
62. East, A.L.L.; Smith, B.J.; Radom, L. Entropies and Free Energies of Protonation and Proton Transfer Reactions. *J. Am. Chem. Soc.* **1997**, *119*, 9014–9020. [[CrossRef](#)]
63. Kabli, S.; van Beelen, E.S.E.; Ingemann, S.; Henriksen, L.; Hammerum, S. The Proton Affinities of Saturated and Unsaturated Heterocyclic Molecules. *Int. J. Mass Spectrom.* **2006**, *249–250*, 370–378. [[CrossRef](#)]
64. Bouchoux, G. Gas Phase Basicities of Polyfunctional Molecules. Part 3: Amino Acids. *Mass Spectrom. Rev.* **2012**, *31*, 391–435. [[CrossRef](#)]
65. Kolboe, S. Proton Affinity Calculations with High Level Methods. *J. Chem. Theory Comput.* **2014**, *10*, 3123–3128. [[CrossRef](#)]

Disclaimer/Publisher's Note: The statements, opinions and data contained in all publications are solely those of the individual author(s) and contributor(s) and not of MDPI and/or the editor(s). MDPI and/or the editor(s) disclaim responsibility for any injury to people or property resulting from any ideas, methods, instructions or products referred to in the content.